J|A|C|S
ARTICLES
Published on Web 05/01/2002

Intramolecular Charge-Transfer Process of Jet-Cooled (*p*-Cyanophenyl)pentamethyldisilane: Roles of the Torsional Motion and the Si−Si Bond Change

Haruki Ishikawa,* Yoichi Shimanuki, Masuyuki Sugiyama, Yuko Tajima, Mitsuo Kira,* and Naohiko Mikami*

Contribution from the Department of Chemistry, Graduate School of Science, Tohoku University, Aoba-ku, Sendai, 980-8578 Japan

Received December 13, 2001

Abstract: To investigate the intramolecular charge-transfer (ICT) process of (*p*-cyanophenyl)pentamethyldisilane (CPDS), laser-induced fluorescence, dispersed fluorescence, and two-color resonance enhanced two-photon ionization spectra were measured in a jet-cooled isolated condition. Dual fluorescence of CPDS was observed from a ground vibrational level in the locally excited $\pi\pi^*$ state. Similar to an emission from the charge-transfer (CT) state in solution, one of the dual emissions of the isolated molecule in the jet was assigned as the CT emission. A significant vibrational dependence on the ICT process was found as exciting vibronic levels of the molecule. It was identified that the promoting mode of the ICT process is a torsional motion of the disilanyl group with respect to the phenyl ring. It was also revealed that an effective appearance energy of the CPDS cation via the CT state is much lower than that via the locally excited $\pi\pi^*$ state suggesting that the electronic configuration of the CT state is similar to that of the cation. On the basis of an electronic configuration of the cationic state, that of the CT state was suggested to be of the (σ_{Si-Si}, 2pπ^*) type.

1. Introduction

Since the first report on dual fluorescence of *p*-(dimethylamino)benzonitrile (DMABN) given by Lippert et al.,[1] intramolecular charge-transfer (ICT) processes have been attractive subjects in the fields of photochemistry, photophysics, physicoorganic chemistry, and so on. Until now, a vast number of studies have been devoted to elucidating the mechanism of this process.[2] The most widely accepted model is the twisted intramolecular charge-transfer (TICT) model, where a 90° twist of the dimethylamino group with respect to the aromatic ring is considered to stabilize the ICT electronic state.[3] For DMABN, several mechanisms other than the TICT model still have been proposed: for example, a pseudo-Jahn−Teller interaction of two energetically close-lying ^1L_a and ^1L_b type benzenic states,[4] an in-plane bending and rehybridization at the acceptor substituent,[5] and a quinoid-type structure model.[6]

To understand the ICT process in condensed phases, we must always take at least two factors into account: the intra- and intermolecular points of view. The former involves a deformation of molecular structure, such as a twist of the electron donor group with respect to the acceptor group. The latter is related to solute−solvent interaction, the so-called solvent effect. Because most of the ICT experiments have been carried out in solution, the ICT state is considered to be stabilized by strong electrostatic interactions between the solute and polar solvents. In solution, even though the ICT state is prepared intramolecularly as a result of a large geometrical change, it is difficult to extract the information about an intrinsic nature of the ICT electronic state. Such a solvent effect cannot be eliminated in solution even if a nonpolar solvent is used. It is desired, therefore, to remove the solvent effect for the investigation of the intramolecular characteristics of the ICT state. Development of supersonic jet techniques combined with the use of laser spectroscopy provides us with the inherent nature of the electronic state of molecules in an isolated condition. In addition, clusters of finite numbers of solvent molecules are also generated in a supersonic jet. Such a molecular cluster is considered to be a microscopic model of solution, so that the intermolecular effects of ICT can be investigated as its cluster-size dependence. In this respect, a number of experimental studies with this technique have been carried out on clusters of ICT molecules such as DMABN[7−11] and 9,9′-bianthryl.[12,13] However, the ICT

(1) (a) Lippert, E. *Z. Naturforsch.* **1955**, *10a*, 541. (b) Lippert, E.; Lüder, W.; Boos, H. In *Advances in Molecular Spectroscopy*; Mangini, A., Ed.; Pergamon: New York, 1962; p 443.
(2) For recent reviews, see: (a) Rettig, W. *Angew. Chem., Int. Ed. Engl.* **1986**, *25*, 971. (b) Bhattacharyya, K.; Chowdhury, M. *Chem. Rev.* **1993**, *93*, 507.
(3) (a) Rotkiewicz, K.; Grellmann, K. H.; Grabowski, Z. R. *Chem. Phys. Lett.* **1973**, *19*, 315. (b) Grabowski, Z. R.; Rotkiewicz, K.; Siemiarczuk, A.; Cowley, D. J.; Baumann, W. *Nouv. J. Chim.* **1979**, *3*, 443.
(4) (a) Zachariasse, K. A.; Harr, T.; Hebecker, A.; Leinhos, U.; Kühnle, W. *Pure Appl. Chem.* **1993**, *65*, 1745. (b) Rettig, W.; Bliss, B.; Dirnberger, K. *Chem. Phys. Lett.* **1999**, *305*, 8.
(5) Sobolewski, A. L.; Domcke, W. *Chem. Phys. Lett.* **1996**, *259*, 119.
(6) Warren, J. A.; Bernstein, E. R.; Seeman, J. I. *J. Chem. Phys.* **1988**, *88*, 871.
(7) Peng, L. W.; Dantus, M.; Zewail, A. H.; Kemniz, K.; Hicks, J. M.; Eisenthal, K. B. *J. Phys. Chem.* **1987**, *91*, 6162.
(8) Howell, R.; Petek, H.; Phillips, D.; Yoshihara, K. *Chem. Phys. Lett.* **1991**, *183*, 249.
(9) Shang, Q.; Bernstein, E. R. *J. Chem. Phys.* **1992**, *97*, 60.

10.1021/ja017753l CCC: $22.00

emission from the isolated monomer has never been observed,[6−10,14−20] and it is believed that the solvation effect must be essential for the ICT emission to occur in this molecule.

Phenylpentamethyldisilane and its derivatives are also known to exhibit the ICT emission in solution.[21−29] Stabilization effects of the ICT state by substitution with an electron-accepting group as well as solvation effects have been reported.[21,22] Concerning the ICT process of the phenyldisilanes, there are two mechanisms that have been proposed. Sakurai and co-workers proposed that the charge transfer occurs from a σ_{Si-Si} orbital to a vacant 2pπ orbital of the phenyl ring, resulting in the (σ_{Si-Si}, 2pπ*) state.[21−23] In their model, the plane involving the disilanyl group is perpendicular to the phenyl ring in the S_0 and locally excited (LE; $\pi\pi$*) states, since there is a conjugation between the σ_{Si-Si} and 2pπ orbitals. The term LE state means the state prepared by the optical excitation from the S_0 state, and a $\pi\pi$* (^1L_b) excited state corresponds to the LE in the present study. A 90° twisting of the disilanyl group with respect to the phenyl ring is considered to break up the conjugation and then stabilize this (σ_{Si-Si}, 2pπ*) state. In this model, the LE state is a perpendicular conformation, whereas the CT state is planar. This situation seems opposite to that of the TICT model. However, the role of the twist is similar to that of the TICT model. Thus, the model proposed by Sakurai and co-workers is considered to be a TICT-like one. On the other hand, Shizuka and co-workers proposed that a (2pπ*, 3dπ_{Si-Si}) state is formed by the electron transfer from the 2pπ* orbital to a vacant 3dπ_{Si-Si} orbital.[24−29] In this model, no twisting is necessary. In their recent work, Shizuka and co-workers reported that conformational changes in the Si-dimethyl group adjacent to the phenyl group play an important role in the ICT process.[30] In the above two mechanisms, roles of the disilanyl and phenyl groups are opposite. In the former model, the electron donor is the disilanyl group, and the acceptor is the phenyl group, whereas the roles are reversed in the latter model.

Among many phenyldisilane derivatives, (*p*-cyanophenyl)-pentamethyldisilane (CPDS) exhibits only the CT emission even in a nonpolar solvent.[22] Thus, the CT state of the compound is expected to lie very close to or below the locally excited (LE) state, so that it is quite suitable for the CT emission to be observed in a jet-cooled condition. To investigate the ICT process of CPDS, we have observed laser-induced fluorescence (LIF), dispersed fluorescence (DF), and two-color resonance enhanced two-photon ionization (two-color RE2PI) spectra of CPDS in the jet-cooled isolated condition. As a result, it was reported in a previous communication that the CPDS monomer exhibits a dual fluorescence even in the jet-cooled isolated condition.[31] In the present paper, we report a detailed analysis of the CT emission of CPDS. The first experimental identification of a presence of a promoting mode for the CT state formation is also described. The promoting mode was assigned as a torsional motion of the disilanyl group with respect to the phenyl ring. In addition, an electronic configuration of the CT state is discussed on the basis of the difference in two-color RE2PI efficiencies between the CT and LE states. Finally, a temporal profile of the CT state is reported, and the rate processes are discussed.

2. Experimental Details

In the present study, a conventional supersonic jet apparatus and a laser system were used. CPDS was synthesized by a method described in ref 22. CPDS was heated to 350 K to gain enough vapor pressure. The CPDS vapor seeded in He gas was supersonically expanded into a vacuum chamber through a pulsed nozzle with an orifice 0.8 mm in diameter. A frequency-doubled output of a tunable dye laser (Lambda Physik FL3002) pumped by a XeCl excimer laser (Lambda Physik LPX105i) was used for the excitation of the jet-cooled CPDS. The laser light irradiated the jet at 10 mm downstream from the nozzle orifice. The fluorescence was collected with a lens placed at the right angle to both the jet and the laser beam, and was detected by a photomultiplier tube (Hamamatsu 1P28). The signal was integrated by a boxcar averager (EG&G Par 4420) and processed by a microcomputer. A 25 cm monochromator (Nikon P250) was placed in front of the photomultiplier tube, when dispersed fluorescence spectra were measured. Slit width was set to 1 mm. In the case of two-color RE2PI spectroscopy, two sets of Nd:YAG pumped tunable dye lasers were used (Continuum Surelite III/LAS LDL 20202; Continuum Powerlite 8000/Continuum ND6000). A delay time between the two laser shots was controlled by a digital delayed pulse generator (SRS DG535). Ions generated were mass-analyzed by a time-of-flight mass spectrometer and then detected by an electron multiplier (Murata). Laser wavelengths were calibrated by an optogalvanic signal from an Fe/Ne hollow cathode lamp.

3. Results

A. Observation of CT Emission from the Jet-Cooled CPDS. Figure 1a shows a LIF spectrum of jet-cooled CPDS observed in the present study. A band origin of the S_1-S_0 transition is located at 35 519.0 cm^{-1}. The bands indicated by asterisks were assigned as those of CPDS$-(H_2O)_{1-2}$ clusters on the basis of both mass analysis and population labeling spectroscopy as described later. An expanded portion near the origin region is inserted in Figure 1b, where a progression of

(10) Howell, R.; Phillips, D.; Petek, H.; Yoshihara, K. *Chem. Phys.* **1994**, *188*, 303.
(11) Howell, R.; Jones, A. C.; Taylor, A. G.; Phillips, D. *Chem. Phys. Lett.* **1989**, *163*, 282.
(12) Honma, K.; Arita, K.; Yamasaki, K.; Kajimoto, O. *J. Chem. Phys.* **1991**, *94*, 3496.
(13) Honma, K.; Kajimoto, O. *J. Chem. Phys.* **1994**, *101*, 1752.
(14) Grassian, V. H.; Warren, J. A.; Bernstein, E. R.; Secor, H. V. *J. Chem. Phys.* **1989**, *90*, 3994.
(15) Bernstein, E. R.; Grassian, V. H.; Warren, J. A. *J. Chem. Phys.* **1990**, *93*, 6910.
(16) Gordon, R. D. *J. Chem. Phys.* **1990**, *93*, 6908.
(17) Kobayashi, T.; Futakami, M.; Kajimoto, O. *Chem. Phys. Lett.* **1986**, *130*, 63.
(18) Gibson, E. M.; Jones, A. C.; Phillips, D. *Chem. Phys. Lett.* **1987**, *136*, 454.
(19) Kajimoto, O.; Yokoyama, H.; Ohshima, Y.; Endo, Y. *Chem. Phys. Lett.* **1991**, *179*, 455.
(20) Kajimoto, O.; Yamasaki, K.; Arita, K.; Hara, K. *Chem. Phys. Lett.* **1986**, *125*, 184.
(21) Sakurai, H.; Sugiyama, H.; Kira, M. *J. Phys. Chem.* **1990**, *94*, 1837.
(22) Kira, M.; Miyazawa, T.; Sugiyama, H.; Yamaguchi, M.; Sakurai, H. *J. Am. Chem. Soc.* **1993**, *115*, 3116.
(23) Kira, M.; Miyazawa, T. In *The Chemistry of Organic Silicon Compounds*; Rappoport, Z., Apeloig, Y., Eds.; John Wiley & Sons: New York, 1998; Vol. 2, Chapter 22.
(24) Shizuka, H.; Obuchi, H.; Ishikawa, M.; Kumada, M. *J. Chem. Soc., Chem. Commun.* **1981**, 405.
(25) Shizuka, H.; Sato, Y.; Ishikawa, M.; Kumada, M. *J. Chem. Soc., Chem. Commun.* **1982**, 439.
(26) Shizuka, H.; Sato, Y.; Ueki, Y.; Ishikawa, M.; Kumada, M. *J. Chem. Soc., Faraday Trans. 1* **1984**, *80*, 341.
(27) Shizuka, H.; Obuchi, H.; Ishikawa, M.; Kumada, M. *J. Chem. Soc., Faraday Trans. 1* **1984**, *80*, 383.
(28) Shizuka, H.; Okazaki, K.; Tanaka, M.; Ishikawa, M.; Sumitani, M.; Yoshihara, K. *Chem. Phys. Lett.* **1985**, *113*, 89.
(29) Hiratsuka, H.; Mori, Y.; Ishikawa, M.; Okazaki, K.; Shizuka, H. *J. Chem. Soc., Faraday Trans. 2* **1985**, *81*, 1665.
(30) Yamamoto, M.; Kudo, T.; Ishikawa, M.; Tobita, S.; Shizuka, H. *J. Phys. Chem. A* **1999**, *103*, 3144.
(31) Tajima, Y.; Ishikawa, H.; Miyazawa, T.; Kira, M.; Mikami, N. *J. Am. Chem. Soc.* **1997**, *119*, 7400.

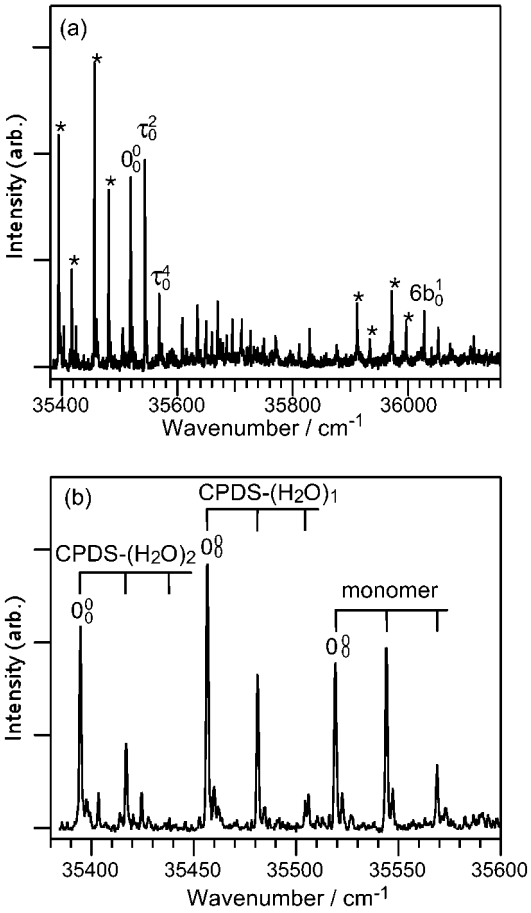

Figure 1. LIF spectrum of the jet-cooled CPDS. A 0_0^0 band is located at 35 519 cm^{-1}. Bands denoted by asterisks belong to the CPDS$-$(H$_2$O)$_{1-2}$ cluster. An expanded portion in the vicinity of the 0_0^0 band is shown in spectrum (b).

25.0 cm^{-1} separation is clearly recognized. Among the dominant bands, a band at the lowest frequency was assigned as the 0_0^0 band. Here, the vibronic bands associated with a low-frequency vibrational mode were tentatively denoted as mode "τ". We assigned this mode as a torsional motion of a disilanyl group with respect to the phenyl ring. A detailed discussion on the assignment of the mode "τ" will be described later. Because the torsional motion should be symmetric with respect to an equilibrium angle and is a nontotally symmetric vibration, as a result, vibrational levels having even quanta of this mode are allowed in the transition from the vibrational ground state due to a symmetry restriction. Thus, the two dominant peaks with a 25 cm^{-1} interval can be assigned as τ_0^2 and τ_0^4, making a short progression due to the torsional mode. A $6b_0^1$ band is located 508.3 cm^{-1} above the band origin. The $6b_0^1$ band is also accompanied by the low-frequency progression, "τ".

Figure 2 shows DF spectra obtained by exciting various levels of the S_1 state. In the figure, spectrum (a) is obtained by the excitation of the 0^0 level, exhibiting a dual emission: an intense emission with distinct vibrational structures starting from the level of the laser excitation and a red-shifted broad emission. To identify a character of the former emission, a high-resolution DF spectrum was measured, as shown in Figure 3. Vibrational assignments and energies of levels observed in the spectrum are summarized in Table 1. The second strongest band is assigned as the 1_1^0 band, where mode 1 is a ring breathing

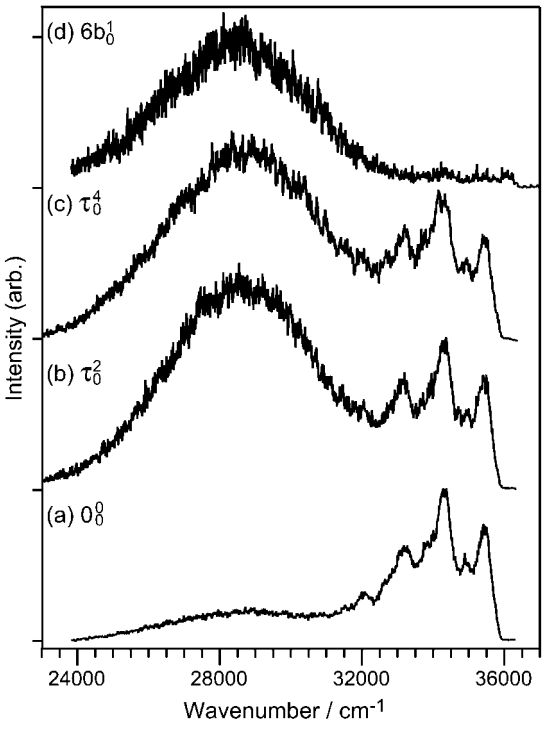

Figure 2. DF spectra of the jet-cooled CPDS. The bands used at the excitation were (a) 0_0^0, (b) τ_0^2, (c) τ_0^4, and (d) $6b_0^1$, respectively.

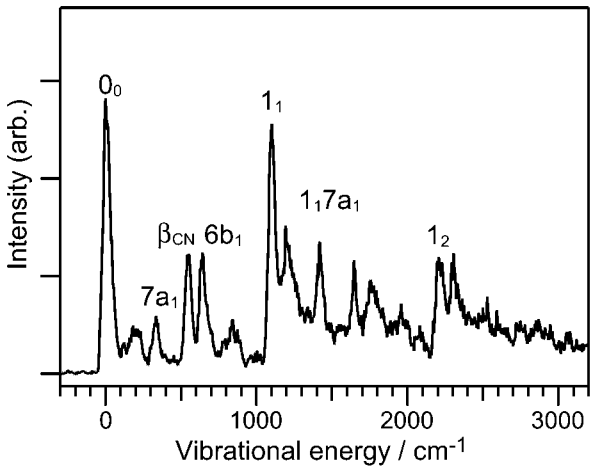

Figure 3. High-resolution DF spectra of the jet-cooled CPDS. The 0_0^0 band was used as the excitation. A horizontal axis is plotted against the vibrational energy in the S_0 state.

motion of a phenyl ring.[32] In addition to transitions to totally symmetric levels such as 1 and 7a, those to nontotally symmetric vibrational levels, 6b and β_{CN}, exhibit rather large intensities. The appearance of the 6b band is interpreted by a vibronic interaction, which is a well-known character of the $\pi\pi^*$ transition of the benzene π system. A vibration of ~550 cm^{-1} is often observed in CN-substituted benzenes, and is assigned to an in-plane bend mode, β_{CN}, of the CN group with respect to the phenyl ring.[32] It is considered that this vibrational level is mixed with the 6b level because these levels have the same symmetry and similar vibrational frequency. This mixing is confirmed by a vibrational analysis based on ab initio MO calculations. Thus, it is explained that the vibronic band to the

(32) Varsányi, G. *Assignments for Vibrational Spectra of Seven Hundred Benzene Derivatives*; Adam Hilger: London, 1974.

Table 1. Vibrational Assignments and Energies of the Levels Observed in the High-Resolution DF Spectrum[a]

E_{vib}/cm^{-1}	assignment
200	
334	7a
550	β_{CN}
648	6b
842	7a + β_{CN}
1100	1
1190	β_{CN} + 6b
1419	1 + 7a
1645	1 + β_{CN}
1756	1 + 6b
2207	1 + 1
2304	1 + β_{CN} + 6b

[a] Notations of the vibrational modes are taken from ref 31.

β_{CN} level appeared in the DF spectrum due to the intensity borrowing from that to the 6b level. Almost all of the sharp bands that appeared in the high-resolution spectrum are related to the vibrational levels in the phenyl moiety. Therefore, the emission with sharp bands is assigned to the emission from the laser pumped LE (2pπ, 2pπ*) state.

For the red-shifted broad emission, the peak maximum, which is located at 28 700 cm^{-1}, exhibited a shift of about 6800 cm^{-1} from the excitation level. This feature is very similar to that of the CT emission of CPDS observed in a nonpolar solvent (ν_{max} = 26 300 cm^{-1}).[22] To distinguish the CT emission from phosphorescence, we have measured the decay of the emission, and it was found that its lifetime is about 15 ns, and is much shorter than a typical decay time of a triplet state. On the basis of a similarity with the CT emission observed in the solution, we assigned this broad emission as a CT emission of CPDS in vapor. It should be noted that CPDS exhibits such a dual emission from the ground vibrational level in the LE state even under a jet-cooled isolated condition. This means that the solvation effect is not necessary for the CT process to occur in the case of CPDS. Moreover, a drastic enhancement of the intensity of the CT emission was observed in the case of the τ_0^2 band excitation (Figure 2b). Despite a very small increase in the excitation energy of only 25 cm^{-1}, the intensity of the CT emission was greatly enhanced. However, an additional excitation of mode "τ", that is, the τ_0^4 band, does not show any drastic change in the DF spectrum as shown in Figure 2c. The result indicates a characteristic level dependence of the CT emission efficiency and the importance of the mode "τ" in the CT process. This is the first experimental identification of the vibrational level dependence on the CT state formation. It is noted that the 0^0 level in the S_1 state has mainly the LE character, whereas the τ^2 level has almost the CT character.

In addition to the vibrational level dependence, an excitation energy effect on the CT state formation was also observed. Figure 2d shows the DF spectrum from the $6b^1$ level, with the excess energy of 508 cm^{-1}. Despite no involvement of the mode "τ" for this level, the intensity of the CT emission is substantially enhanced, and the LE emission is extremely weak. In addition, the DF spectrum from the $6b^1\tau^2$ level was found to be quite similar to that from the $6b^1$ level, showing no substantial mode "τ" dependence of the ICT emission yield. It is considered that the fast intramolecular vibrational energy redistribution (IVR) in the S_1 state makes the effect of the mode "τ" dependence unclear, in the relatively high excess energy region.

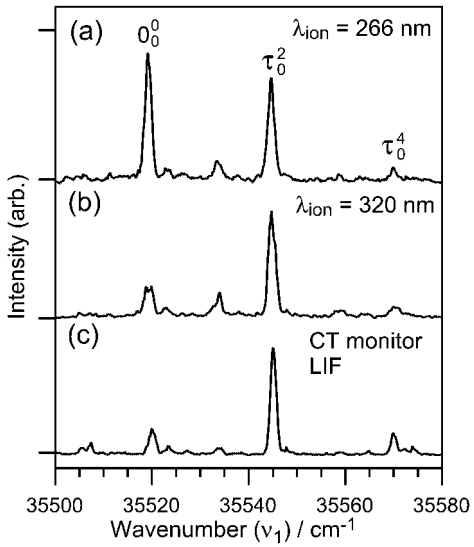

Figure 4. Two-color RE2PI spectra of CPDS. The wavelength of the ionization laser light is indicated in the figure. A LIF spectrum monitoring only the CT emission is displayed in the bottom for comparison.

B. Two-Color RE2PI Spectrum of CPDS. When we observed the REMPI spectra of CPDS in the origin region, we have noticed an anomaly of the intensity distribution among the 0_0^0, τ_0^2, and τ_0^4 bands. Two-color RE2PI spectra of CPDS were also measured and compared with the LIF spectrum obtained by monitoring the CT emission part. Figure 4 shows two-color RE2PI spectra of CPDS in the origin region of the S_1-S_0 transition; the spectra (a) and (b) were measured with the ionization laser wavelength (λ_{ion}) of 266 and 320 nm, respectively. It is apparent that the relative intensity of the vibronic bands, the τ_0^2 band especially, with respect to the 0_0^0 band depends on λ_{ion}; in spectrum (a), the 0_0^0 band is as intense as the τ_0^2 band, showing the similar spectral feature to the LIF spectrum obtained by monitoring the total emission (Figure 1b). In spectrum (b) of Figure 4, on the contrary, the intensity of the 0_0^0 band becomes much weaker than that of the τ_0^2 band. The result indicates that the yield of two-color RE2PI is not constant for each band with respect to λ_{ion}. Thus, we observed the ionization yield spectra of CPDS via the 0_0^0 and the τ_0^2 bands, as shown in Figure 5. Ionization yield via the τ_0^2 band remains almost unchanged in an energy region plotted, whereas that via the 0_0^0 band substantially decreases as the ionization energy becomes smaller. This means that the appearance energy of the CPDS cation via the τ_0^2 band is substantially lower than that via the τ_0^2 band. As mentioned above, the vibronic level τ^2 in S_1 exhibits a dominant character of the CT state, while the S_1 origin 0^0 has a less CT character. In this respect, the difference in the appearance energy of the ionization yield spectra corresponds to the difference in the CT character. As will be discussed later, the ionic state which is accessed with lower ionization energy is characterized to be the state having a favorable Franck−Condon region from the CT state of the neutral CPDS.

Considering the above, one may easily find the reason the intensity of the 0_0^0 band is substantially weaker than that of the τ_0^2 vibronic band in the two-color RE2PI spectrum with λ_{ion} = 320 nm, which corresponds to the total photoionization energy of 8.27 eV. Because the difference in the vibronic band intensity originates from the difference in the CT character, we also

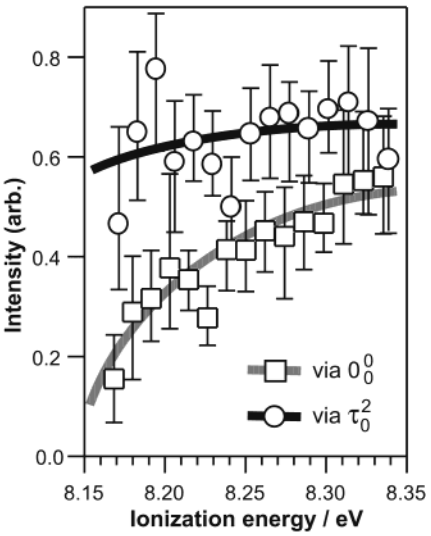

Figure 5. Relative efficiencies of the two-color RE2PI via the 0^0 (□) and the τ^2 (○) levels in the S_1 state.

observed the LIF spectrum measured by monitoring only the CT emission, as shown in Figure 4c. Relative intensities between the 0_0^0 and the τ_0^2 bands in Figure 4c are very similar to those in Figure 4b. Because the relative intensities in Figure 4c represent relative yields of the CT state, this similarity indicates that the ionization laser light at $\lambda_{ion} = 320$ nm picks up molecules in the CT state preferentially. The ionization energy dependence indicates that the appearance energy of the cation via the CT state is much lower in energy than that via the LE state. This behavior should carry the information about the electronic configuration of the CT state as discussed later.

C. Solvated Cluster of CPDS with Water. As indicated in Figure 1b, we assigned band origins of the CPDS−$(H_2O)_1$ and the CPDS−$(H_2O)_2$ clusters. The number of the attached water molecules was determined by the mass analysis. The amounts of the red-shift of origin bands of the (1:1) and (1:2) clusters measured from that of the monomer are 62.5 and 124.7 cm^{-1}, respectively. A similar pattern of the LIF spectrum was observed in the case of benzonitrile clusters with water, with red-shifts of 70.2 and 139.5 cm^{-1} for the (1:1) and (1:2) clusters, respectively.[33] Thus, the CPDS−water clusters are expected to have a similar structure to those of the benzonitrile−water clusters. In the case of the benzonitrile−water clusters, water molecules are known to be found at the CN site through a hydrogen bond. The fact that the progressions of the mode "τ" are still clearly seen for the CPDS−water clusters indicates that attached water molecules do not disturb the torsional motion of CPDS. This also supports the similarity of the cluster structure between the CPDS and benzonitrile.

Figure 6 shows DF spectra of the CPDS−water clusters. Contrary to the case of the CPDS monomer, only the CT emission was observed in the case of the clusters. No LE emission was observed. This means that the solvation of a small number of water molecules accelerates the ICT process. In addition, the solvation leads to an increase of the red-shift of the peak maximum of the CT emission measured from the laser excited level. The amounts of the red-shifts are 7900 and 8800 cm^{-1} for the (1:1) and (1:2) clusters, respectively. As the number

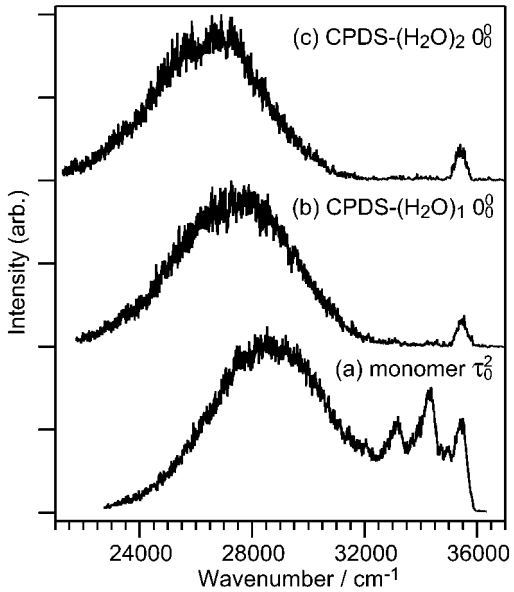

Figure 6. DF spectra of the solvated CPDS clusters with water molecules. (a) CPDS−$(H_2O)_1$, (b) CPDS−$(H_2O)_2$, (c) CPDS monomer. The bands used at the excitation were for (a) and (b), τ_0^2 for (c), respectively.

of the water molecule increases, the amount of the red-shift also increases by about 1000 cm^{-1}. Such a large change in the red-shift is a clear indication of the stabilization of the CT state by the solvation. These two features, the acceleration of the ICT process and the stabilization of the CT state, are a clear indication of a microscopic solvation effect. The ICT processes of solvated clusters of CPDS with other solvents were also investigated and will be reported elsewhere.[34]

D. Ab Initio MO Calculations of Neutral and Cationic States of CPDS. To interpret the CT character difference of the appearance energy of the CPDS cation, we have carried out ab initio molecular orbital (MO) calculations of the neutral (S_0) and cationic (D_0) states using a Gaussian 98 program package.[35] An optimized structure for each state was obtained at RHF or UHF level with 6-31G(d) basis set, for S_0 or D_0, respectively. Bond lengths and angles in the optimized geometry for each state are listed in Table 2. Figure 7a shows a position of each atom listed in Table 2. In the case of S_0, it was found that the perpendicular conformation, where the disilanyl group lies in a plane perpendicular to the phenyl ring, corresponds to a global minimum. A planar conformation, where the disilanyl group lies in a plane containing the phenyl ring, is located 523 cm^{-1} higher in energy than the perpendicular one. Figure 8 shows potential curves of S_0 and D_0 along the torsional angle. At each point, only the torsional angle was fixed, and the remaining coordinates were optimized. It is suggested that only the perpendicular conformation exists in a jet-cooled condition,

(33) Ishikawa, S.; Ebata, T.; Mikami, N. *J. Chem. Phys.* **1999**, 9504.

(34) Shimanuki, Y.; Ishikawa, H.; Tajima, Y.; Kira, M.; Mikami, N., in preparation.

(35) Frisch, M. J.; Trucks, G. W.; Schlegel, H. B.; Scuseria, G. E.; Robb, M. A.; Cheeseman, J. R.; Zakrzewski, V. G.; Montgomery, J. A., Jr.; Stratmann, R. E.; Burant, J. C.; Dapprich, S.; Millam, J. M.; Daniels, A. D.; Kudin, K. N.; Strain, M. C.; Farkas, O.; Tomasi, J.; Barone, V.; Cossi, M.; Cammi, R.; Mennucci, B.; Pomelli, C.; Adamo, C.; Clifford, S.; Ochterski, J.; Petersson, G. A.; Ayala, P. Y.; Cui, Q.; Morokuma, K.; Malick, D. K.; Rabuck, A. D.; Raghavachari, K.; Foresman, J. B.; Cioslowski, J.; Ortiz, J. V.; Stefanov, B. B.; Liu, G.; Liashenko, A.; Piskorz, P.; Komaromi, I.; Gomperts, R.; Martin, R. L.; Fox, D. J.; Keith, T.; Al-Laham, M. A.; Peng, C. Y.; Nanayakkara, A.; Gonzalez, C.; Challacombe, M.; Gill, P. M. W.; Johnson, B. G.; Chen, W.; Wong, M. W.; Andres, J. L.; Head-Gordon, M.; Replogle, E. S.; Pople, J. A. *Gaussian 98*, revision A.7; Gaussian, Inc.: Pittsburgh, PA, 1998.

Table 2. Optimized Geometry of the D_0 and the S_0 States of CPDS

	D_0	S_0		D_0	S_0
bond lengths			bond angles		
C_1-C_2	1.400	1.397	$C_1-Si_9-Si_{10}$	101.397	108.962
C_2-C_3	1.382	1.382	$C_1-Si_9-C_{11}$	116.458	108.610
C_3-C_4	1.391	1.389	$C_{11}-Si_9-C_{11}'$	115.596	108.380
			$Si_{10}-Si_9-C_{11}$	101.444	111.109
C_2-H_7	1.075	1.075	$Si_9-Si_{10}-C_{12}$	102.161	110.010
C_3-H_8	1.073	1.074	$Si_9-Si_{10}-C_{13}$	101.651	110.066
			$C_{12}-Si_{10}-C_{12}'$	115.851	109.029
C_4-C_5	1.444	1.445	$C_{12}-Si_{10}-C_{13}$	115.773	108.857
C_5-N_6	1.135	1.137			
C_1-Si_9	1.858	1.911	dihedral angle		
Si_9-Si_{10}	2.726	2.371	$C_2-C_1-Si_9-Si_{10}$	90.713	89.851
Si_9-C_{11}	1.871	1.899			
$Si_{10}-C_{12}$	1.870	1.900			
$Si_{10}-C_{13}$	1.872	1.900			

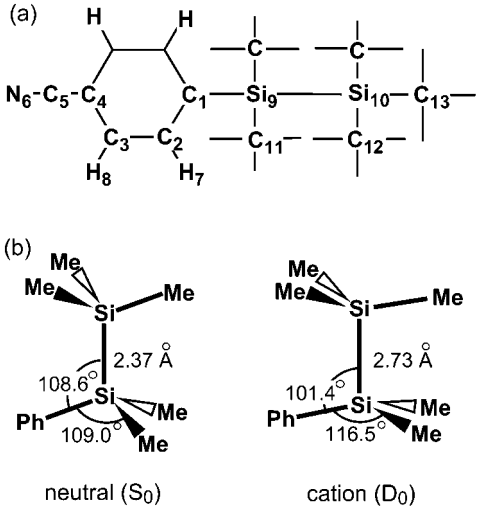

Figure 7. (a) Atom notation of CPDS. All the methyl groups are omitted. (b) Schematic representation of the optimized geometries of the disilanyl group in both the S_0 and the D_0 states.

because of a substantial energy difference from the other. A very recent analysis of the rotational envelope of a high-resolution LIF of a jet-cooled PDS clearly exhibited that the perpendicular conformation is a dominant species in the jet-cooled condition.[38] Although the level of our calculation was not high enough to discuss exact barrier height, the above analysis of PDS also supports that the perpendicular conformation is the most stable in the case of CPDS. It is also noted that a curvature near the minimum of S_0 is very small and that the amplitude of the torsional motion is quite large, even for a small quantum number state.

The structure of the cyanophenyl group and the methyl groups remains essentially unchanged upon ionization. Each methyl group takes a tetrahedral structure and is oriented so that the steric repulsion among the methyl groups is minimized. On the contrary, the structure of the disilanyl group in D_0 is substantially different from that in S_0 as shown schematically in Figure 7b. The Si−Si bond length is 2.73 Å in D_0, whereas it becomes 2.37 Å in S_0, corresponding to that the Si−Si bonding orbital, σ_{Si-Si}, is half-filled in D_0. Actually, a SOMO obtained by the

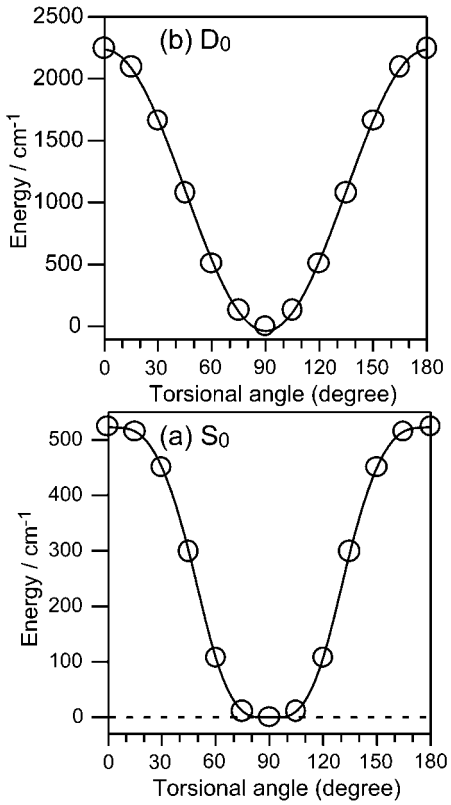

Figure 8. Potential energy curve along the torsional coordinate for (a) the S_0 and (b) the D_0 states obtained by the ab initio MO calculation.

ab initio calculation is shown to be of a σ_{Si-Si} type. In addition to the elongation of the Si−Si bond, the bond angles at both of the Si atoms are altered drastically upon ionization. In S_0, each Si atom takes a sp^3 hybridization; because all of the values of each C−Si−C and Si−Si−C bond angle are ∼109°, that is a tetrahedral structure. On the other hand, the bonding structures around the Si atoms are not tetrahedral anymore in D_0. The values of three C−Si−C bond angles are 115° and Si−Si−C angles are 100°. This structure indicates that the hybridization of the Si atoms in the D_0 becomes sp^2-like and the half-filled Si−Si bonding orbital consists of 3p orbitals of the Si atoms.

4. Discussions

A. Assignment of the Low-Frequency Mode "*τ*". It was revealed that the low-frequency mode "τ" plays an important role in the CT state formation. Therefore, an assignment of the mode "τ" is of particular significance in this study. A similar low-frequency progression was observed in the MPI spectrum of phenylpentamethyldisilane (h_5-PDS).[36] The most probable assignment of this mode appearing commonly in phenyldisilanes is a torsional motion of the disilanyl group with respect to the phenyl ring. An isotope effect on the vibrational frequency should provide a plausible assignment of the mode "τ". It was expected that a deuteration of hydrogen atoms in the phenyl ring (d_5-PDS) is the most effective way to assign whether the mode "τ" is a torsional motion or not. The deuteration of hydrogen atoms in the phenyl ring affects not only vibrational modes which are localized on the phenyl ring but also relative motion of the disilanyl group with respect to the phenyl ring. However, the phenyl ring itself does not have a low-frequency mode, whose frequency is below 50 cm^{-1}. Therefore, if the

(36) Kira, M.; Miyazawa, T.; Mikami, N.; Sakurai, H. *Organometallics* **1991**, *11*, 3793.
(37) Tsutsui, Y.; Wasada, H. *Chem. Lett.* **1995**, 517.
(38) Ishikawa, H.; Sugiyama, M.; Kishi, T.; Kira, M.; Mikami, N.; Kajimoto, O.; Reddy, A. M. *Chem. Phys.*, in press.

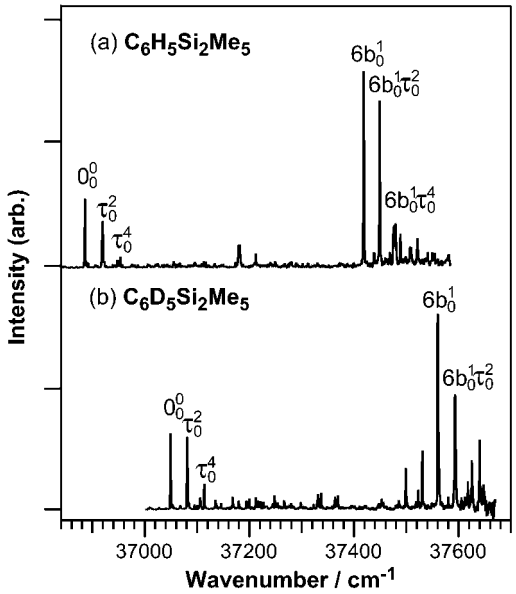

Figure 9. LIF spectra of (a) h_5-PDS and (b) d_5-PDS.

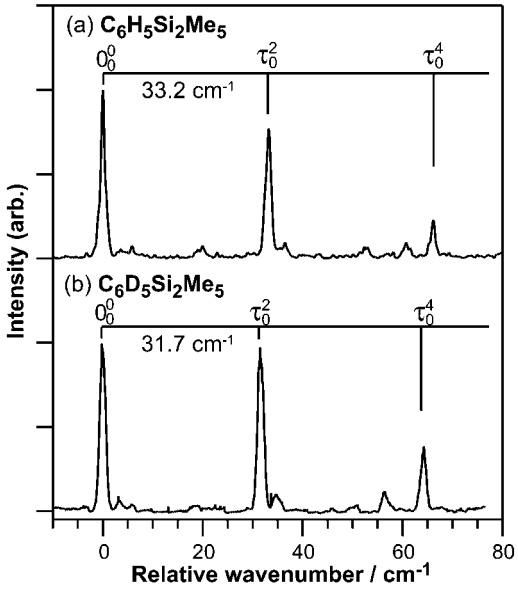

Figure 10. Comparison of the low-frequency mode "τ" between (a) h_5-PDS and (b) d_5-PDS. The abscissa represents relative wavenumbers from each 0_0^0 band.

frequency of the mode "τ" would change by the deuteration, we could assign the mode "τ" as the relative motion of the disilanyl group with respect to the phenyl ring.

Figure 9 shows LIF spectra of h_5-PDS and d_5-PDS observed in the present study. The 0_0^0 band of d_5-PDS is located at 37 049.3 cm^{-1}, which is blue-shifted by 163.5 cm^{-1} as compared to that of the h_5-PDS (36 885.8 cm^{-1}). An expanded portion near the 0_0^0 band is shown in Figure 10. Frequencies of the mode "τ" are 33.2 and 31.7 cm^{-1} for h_5-PDS and d_5-PDS, respectively. The frequency of the mode "τ" is reduced by 1.5 cm^{-1} (ca. 4.5% frequency change) by the deuteration of the phenyl ring. A frequency change of ca. 8% is predicted by the ab initio calculation for h_5-PDS and d_5-PDS. This suggests that the mode "τ" corresponds to a relative motion of the disilanyl group with respect to the phenyl ring. There are three kinds of relative motions of the disilanyl group with respect to the phenyl ring: stretch, bending, and torsion. Among them, the frequency of the torsional motion must be the lowest. Thus, we assigned the mode "τ" to be the torsional motion of the disilanyl group with respect to the phenyl ring.

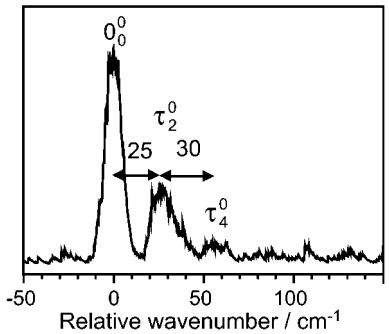

Figure 11. High-resolution DF spectrum of CPDS in the vicinity of the 0_0^0 band. A 0.75 m monochromator was used in this measurement. A short progression of mode "τ" is observed.

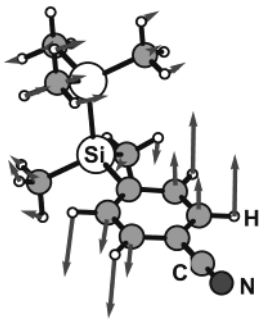

Figure 12. Vector model of the lowest frequency mode of CPDS obtained by the ab initio MO calculation. Because the mass of the disilanyl group is heavier than that of the phenyl ring, it is seen that the phenyl ring rotates around the $Si-C_{phenyl}$ bond, whereas the disilanyl group does not move. This figure was prepared using a program in ref 37.

In addition to the above discussion on the assignment of the mode "τ", we compared its frequency in S_0 with that estimated by an ab initio MO calculation. Figure 11 shows a high-resolution DF spectrum in the vicinity of the 0_0^0 band. A low frequency progression is clearly seen. This progression corresponds to the mode "τ" in the fluorescence excitation spectrum. Contrary to the LE state, the interval is not harmonic. The interval between the 0_0^0 and τ_2^0 bands is 25 cm^{-1}, whereas that between the τ_2^0 and τ_4^0 is 30 cm^{-1}. This indicates that the torsional potential of S_0 is a bit anharmonic. Thus, the frequency of the mode "τ" in S_0 is at most 12.5 cm^{-1}. The calculated vibrational frequency of the torsional motion was obtained to be 8.9 cm^{-1} by the HF/6-31G(d) ab initio MO calculation, which reproduces the experimentally obtained frequency. An optimized geometry obtained in the calculation will be described later together with that of a cationic CPDS. A vector representation of the mode "τ" is shown in Figure 12. It is clearly seen that the mode "τ" mainly consists of a torsional motion of the phenyl ring and a little contribution of methyl group. Thus, our assignment was confirmed both experimentally and theoretically.

B. Electronic Characterization of the LE and CT States. In the case of PDS, it is noticed that the intensity of the $6b_0^1$ band of the LIF spectrum is much larger than that of the 0_0^0 band as shown in Figure 9. In addition, rotational band contours of the 0_0^0 and the $6b_0^1$ bands show different transition types with each other.[38] These features can be interpreted by a vibronic

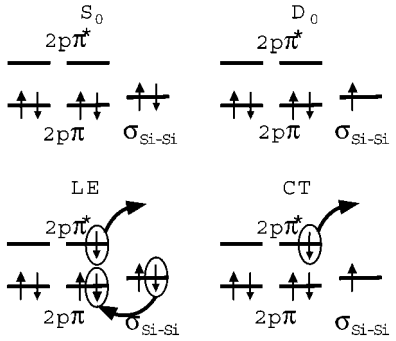

Figure 13. Electronic configuration of S_0, LE, CT, and D_0 states of CPDS.

coupling that is similar to that in the case of the S_1-S_0 transition of benzene. This indicates that the electronic transition of PDS preserves the symmetry forbidden character of the $\pi\pi^*$ ($^1B_{2u}-{}^1A_{1g}$) transition of benzene. In the case of CPDS, on the other hand, the intensity of the $6b_0^1$ band is substantially weaker than in the case of PDS, showing that the CN substitution reduces the forbidden character. Nevertheless, the common appearance of the $6b_0^1$ band for both of the molecules indicates that the electronic character of the S_1 (LE) state is that of the $\pi\pi^*$ excitation which is localized at the phenyl π system.

Major electronic configurations representing the S_0, LE, CT, and D_0 states are schematically shown in Figure 13. All of the $2p\pi$ and the σ_{Si-Si} orbitals are filled by electrons in S_0, while an electron in the $2p\pi$ orbitals is excited to the $2p\pi^*$ orbital to form the LE ($2p\pi$, $2p\pi^*$) state. As described above, the ab initio MO calculation reveals that the σ_{Si-Si} orbital is half-filled, whereas the $2p\pi$ orbitals are fully filled in D_0, characterizing that the first ionization energy is due an electron loss not from the phenyl ring but from the Si−Si bond. Comparing the electronic configuration of the LE state with that of D_0, it is indicated that the ionization to D_0 via the LE state requires the electron transfer from the σ_{Si-Si} to the $2p\pi$ orbitals as well as a removal of an electron in the $2p\pi^*$ orbital as indicated in Figure 13. Such a rearrangement in the electron configuration may result in a substantial geometrical change upon ionization. On the other hand, the ionization via the CT state requires only a removal of an electron in the $2p\pi^*$ orbital, as far as the electronic configuration of the CT state is assumed, as shown in Figure 13. In this case, large geometrical changes upon ionization are not expected to occur, so that the FC region upon the ionization from the CT state may not be so different from the equilibrium of the CT state. This assumption well explained the fact that the appearance energy of the cation via the CT state is much lower in energy than that via the LE state as described above. Thus, the two-color RE2PI ionization spectrum strongly suggests that the electronic character of the CT state of CPDS is a (σ_{Si-Si}, $2p\pi^*$) type state. The CT process from the LE states is described as the electron transfer from the σ_{Si-Si} to the half-filled $2p\pi$ orbitals in the LE state. That is, the disilanyl and the cyanophenyl group act as an electron donor and an acceptor in the CT process, respectively.

C. Mechanism of the CT Process: Torsional Motion as a Promoting Mode of the CT Process. As mentioned above, the torsional mode "τ" plays an important role in the CT process. According to Fermi's golden rule, a rate constant for the CT process, $k_{LE\rightarrow CT}$, should depend on the interaction matrix element between the LE and the CT states, $\langle\Psi_{LE}|\hat{H}|\Psi_{CT}\rangle$, and the density of states in the CT state, ρ. Accordingly,

$$k_{LE\rightarrow CT} = \frac{2\pi}{h}\langle\Psi_{LE}|\hat{H}|\Psi_{CT}\rangle^2\rho \qquad (1)$$

where $\Psi_{LE\text{ or }CT}$ represents a vibronic wave function in each electronic state.

Let us consider first a dependence of ρ on $k_{LE\rightarrow CT}$. The red-shift of the CT emission measured from the excitation wavenumber was about 7000 cm^{-1}. Because our observation was carried out in a collision-free condition, there is no energy relaxation except for a radiative process. Thus, such a large red-shift implies that the emitting levels in the CT state should have a vibrational excess energy of several thousand wavenumbers, even though the emission terminates at the considerably high-energy Franck−Condon region of S_0. The value of ρ at such large excess energy levels in the CT states should be so large that a small increase in the vibrational energy of only 25 cm^{-1} does not cause a substantial change in ρ. Thus, it is unlikely that the remarkable change in $k_{LE\rightarrow CT}$ would be due to the change of ρ. Therefore, we conclude that the significant change in the CT emission intensity by the excitation of the mode "τ" comes from a change in the interaction matrix element, $\langle\Psi_{LE}|\hat{H}|\Psi_{CT}\rangle$.

Next, the interaction between the LE and the CT states in terms of nonadiabatic interaction is considered. Because the spin state in both states is singlet, the ICT process of CPDS can be treated as a process of internal conversion (IC). In general treatment for the IC process, the interaction matrix element can be expressed as

$$\begin{aligned}\langle\Psi_{LE}(\mathbf{q},\mathbf{Q})|\hat{H}|\Psi_{CT}(\mathbf{q},\mathbf{Q})\rangle &= \sum_k \left\langle \phi_{LE}(\mathbf{q},\mathbf{Q})\left|\left\langle \chi_{LE}(\mathbf{Q})\left|\frac{\partial^2}{\partial Q_k^2}\right|\phi_{CT}(\mathbf{q},\mathbf{Q})\right\rangle\right|\chi_{CT}(\mathbf{Q})\right\rangle \\ &\approx \sum_k \left\langle \chi_{LE}(\mathbf{Q})\left|\left\{\left\langle \phi_{LE}(\mathbf{q},\mathbf{Q})\left|\frac{\partial}{\partial Q_k}\right|\right.\right.\right. \times \\ &\qquad \left.\left.\left.\phi_{CT}(\mathbf{q},\mathbf{Q})\right\rangle\right\}\frac{\partial}{\partial Q_k}\right|\chi_{CT}(\mathbf{Q})\right\rangle \qquad (2)\end{aligned}$$

where $|\phi_{LE\text{ or }CT}(\mathbf{q},\mathbf{Q})\rangle$ and $|\chi_{LE\text{ or }CT}(\mathbf{Q})\rangle$ represent electronic and vibrational wave functions of the LE or CT states, respectively.[39] Coordinates $\mathbf{q}$ and $\mathbf{Q}$ are those of electrons and vibrational modes, respectively. A vibrational mode "k" which has a nonzero value of the matrix element

$$\left\langle \phi_{LE}(\mathbf{q},\mathbf{Q})\left|\frac{\partial}{\partial Q_k}\right|\phi_{CT}(\mathbf{q},\mathbf{Q})\right\rangle$$

is referred to as a promoting mode.

In the previous section, the electronic configurations of the LE and CT states are characterized as the ($2p\pi$, $2p\pi^*$) and the (σ_{Si-Si}, $2p\pi^*$) types, respectively. In the ICT process, an electron in the σ_{Si-Si} orbital is transferred into the half-filled $2p\pi$ orbital. In evaluating the matrix element, the dependence of these MOs with respect to the torsional angle should be very important, so that we examined the characteristic of these MOs on the basis of the results of ab initio theoretical calculations. Although MOs

(39) Henry, B. R.; Siebrand, W. In *Organic Molecular Photophysics*; Birks, J. B., Ed.; John Wiley & Sons: New York, 1973; Vol. 1, Chapter 4, p 185.

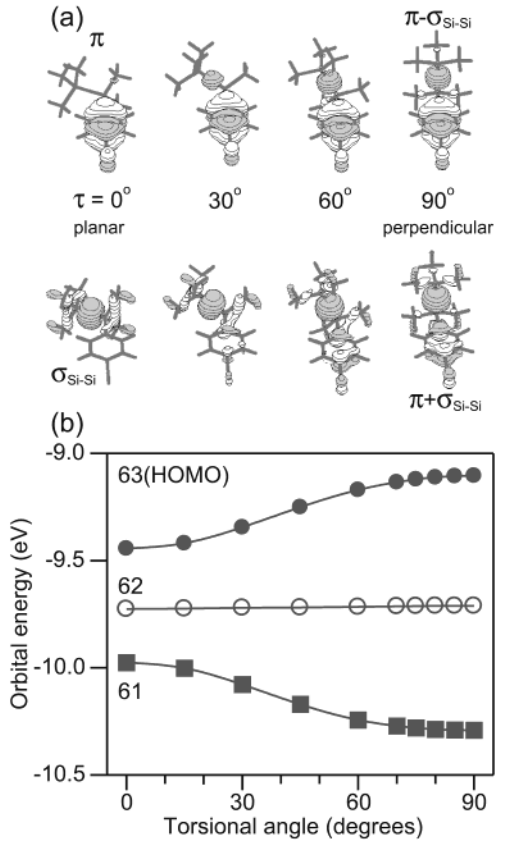

Figure 14. Torsional angle dependence of (a) molecular orbitals and (b) their energies which are related to the 2pπ and σ_{Si-Si} orbitals. The numbers 61, 62, and 63 indicate order of orbitals from the bottom. The 63rd orbital corresponds to HOMO. The 62nd orbital corresponds to another 2pπ orbital that has a node perpendicular to the Si−C_{phenyl} bond.

examined here were obtained by calculations for the electronic ground state, the results should provide us with a qualitative picture of the interaction between the 2pπ and σ_{Si-Si} orbitals. Figure 14a shows a torsional angle dependence of the 2pπ and σ_{Si-Si} orbitals. In the planar configuration, the HOMO orbital is of a pure 2pπ. On the other hand, the 2pπ and σ_{Si-Si} orbitals are mixed with each other in the perpendicular configuration. Their mixing ratio depends on the torsional angle "θ" as shown in Figure 14a. Torsional angle dependences of these orbital energies are plotted as shown in Figure 14b. It is noted that the difference in energy between the 63rd (HOMO) and 61st orbitals increases with the torsional angle. This energy repelling between these orbitals indicates an interaction between these orbitals. This result indicates that the interaction matrix element

$$\left\langle \phi_{LE}(\mathbf{q},\mathbf{Q}) \left| \frac{\partial}{\partial Q_\tau} \right| \phi_{CT}(\mathbf{q},\mathbf{Q}) \right\rangle$$

should have an appreciable value and that the vibrational mode "τ" is a promoting mode of the ICT process of CPDS.

Symmetry consideration to this process also supports the above discussion. The CPDS molecule in its equilibrium configuration, which is perpendicular, has a C_s symmetry. In this case, the plane of reflection contains the Si−Si bond and CN group, and is perpendicular to the phenyl ring. On this symmetry, the electronic symmetry of the LE state is considered to be a″, since the transition dipole moment of the $\pi\pi^*$ transition lies perpendicular to the reflection plane. On the other hand,

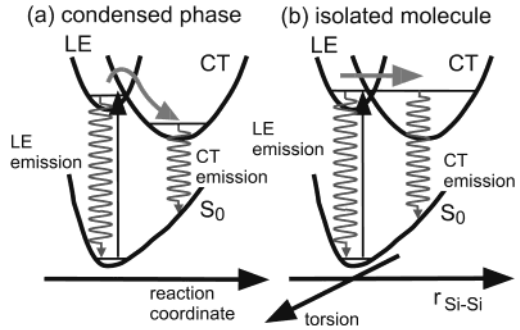

Figure 15. Schematic representation of the ICT processes in the (a) condensed phase and (b) isolated molecular condition.

the CT state has a′ symmetry, since both the half-filled σ_{Si-Si} and the π^* orbitals have a′ symmetry. Thus, it is necessary that Q_k in the eq 2 must be of a″ symmetry, otherwise the integral in eq 2 vanishes. The torsional motion satisfies this symmetry requirement.

By assuming that the value of the matrix element

$$\left\langle \phi_{LE}(\mathbf{q},\mathbf{Q}) \left| \frac{\partial}{\partial Q_\tau} \right| \phi_{CT}(\mathbf{q},\mathbf{Q}) \right\rangle$$

does not largely change with **Q**, eq 2 can be rewritten as

$$\langle \Psi_{LE}(\mathbf{q},\mathbf{Q}) | \hat{H} | \Psi_{CT}(\mathbf{q},\mathbf{Q}) \rangle \approx \left\{ \left\langle \phi_{LE}(\mathbf{q},\mathbf{Q}_0) \left| \frac{\partial}{\partial Q_\tau} \right| \phi_{CT}(\mathbf{q},\mathbf{Q}_0) \right\rangle \right\} \left\langle \chi_{LE}(Q_\tau) \left| \frac{\partial}{\partial Q_\tau} \right| \chi_{CT}(Q_\tau) \right\rangle \langle \chi_{LE}(\mathbf{Q}') | \chi_{CT}(\mathbf{Q}') \rangle \quad (3)$$

where $\mathbf{Q}'$ represents a set of vibrational coordinates except for the torsional mode "τ". In this respect, the drastic change in the I_{CT}/I_{LE} ratio with respect to the quantum number of "τ" can be explained as a result of the variation of the vibrational overlap term

$$\left\langle \chi_{LE}(Q_\tau) \left| \frac{\partial}{\partial Q_\tau} \right| \chi_{CT}(Q_\tau) \right\rangle$$

in eq 3. The last term in eq 3 represents the vibrational overlap integral along all the vibrational coordinates except for the mode "τ". This integral depends on the vibrational modes which are associated with the structural difference between the LE and the CT states and are called accepting modes.

The structural similarity between the CT and D_0 states was suggested as mentioned in sections 3B and 4B. Both states have an unpaired electron in the σ_{Si-Si} orbital; a local structure of the disilanyl group should be similar to each other. Because the electronic configuration of the LE state is the $\pi\pi^*$ type, there is no substantial structural change in the disilanyl group associating with the $\pi\pi^*$ excitation. Thus, the major structural change between the LE and the CT state should be localized in the disilanyl group. On the basis of the equilibrium structure obtained by the ab initio MO calculation, it is expected that the most probable candidate of the accepting mode is a Si−Si stretching vibration. Other candidates of the accepting mode are changes in the bond angles around Si atoms due to the change in the hybridization of the orbitals at the Si atom from sp^3-like to sp^2-like.

In general, the ICT process is described on the basis of potential curves shown in Figure 15a. The horizontal axis

represents a so-called reaction coordinate. The term "reaction coordinate" is often used for accounting for the transition from the LE to the CT state and also for the large Stokes shift. It is assumed that the LE state has a similar equilibrium structure to that of the S_0 state. Thus, the LE emission spectrum exhibits a so-called mirror image of the absorption spectrum. On the other hand, there is a substantial structural difference between the CT and the S_0 or LE states. Therefore, the Franck−Condon region of the CT → S_0 emission appears in a much longer wavelength region as compared with that of the LE emission. In ICT process in solution, the reaction coordinate consists of both the intramolecular structural change and the change in the solvation coordinate; these two effects are not easily separated in the condensed phase experiments. In the present experiments in the jet, however, the reaction coordinate consists of only the intramolecular structure, since our observation was carried out in an isolated molecular condition without solvation. As discussed above, both the promoting and the accepting modes play important roles in the ICT process of the CPDS, and they are the most inherent part of the reaction coordinate of ICT. The structural change in the ICT process discussed here should be related to the change in hybridization at the Si atom.

From a viewpoint in the above scheme, one can describe the ICT process of CPDS as follows. First, the transition from the LE to the CT states is promoted by the torsional motion, and then the vibrational relaxation along the Si−Si bond stretch motion occurs in the CT state leading to the Stokes-shifted emission (see Figure 15b). However, since the ICT process that we observed occurs in a jet-cooled isolated molecular condition, the following two points must be noted. The first point concerns the transition from the LE to the CT states. Alternative representation of this process is that the LE and the CT states are mixed by the term in eq 2, which is neglected in the Born−Oppenheimer approximation. Because the magnitude of the interaction between the LE and the CT states is determined by the vibrational overlap term

$$\left\langle \chi_{\mathrm{LE}}(Q_\tau)\left|\frac{\partial}{\partial Q_\tau}\right|\chi_{\mathrm{CT}}(Q_\tau)\right\rangle,$$

there is no necessity of the large amplitude torsion. The second point is that there is no energy relaxation except for the radiative decay. Thus, the vibrational relaxation in the CT state corresponds to the intramolecular vibrational energy redistribution (IVR) process. When the extensive IVR occurs, the transition from these levels exhibits a broad profile, the band center of which corresponds to the Franck−Condon accessible region in S_0 from the minimum of the CT state. As a result, the large Stokes shift of the CT emission observed in the present study becomes similar to that observed in the condensed phase. As mentioned above, the large Stokes shift can be associated with the substantial structural difference between the CT and the S_0 states. In many TICT models, it is generally accepted that the structural change along with the torsional coordinate is responsible for the large Stokes shift. However, the present experiment shows that it is not the case for the ICT process of CPDS. Because the torsional barrier is calculated to be about 500 cm^{-1} in S_0, this value is not large enough to explain the large Stokes shift of several thousand wavenumbers. On the other hand, the ab initio calculation shows that an elongation of the Si−Si distance makes the potential energy higher by thousands of wavenumbers. Thus, the Si−Si stretch vibration is considered to be the most likely candidate for the vibrational mode that is associated with the large Stokes shift of the CT emission. In the case of polysilanes such as Si_4Me_{10}, Si_5Me_{12}, and Si_6Me_{14}, Michl and co-workers have proposed a similar interpretation in which a large Stokes shift is associated with a large Si−Si bond elongation in the upper state.[40]

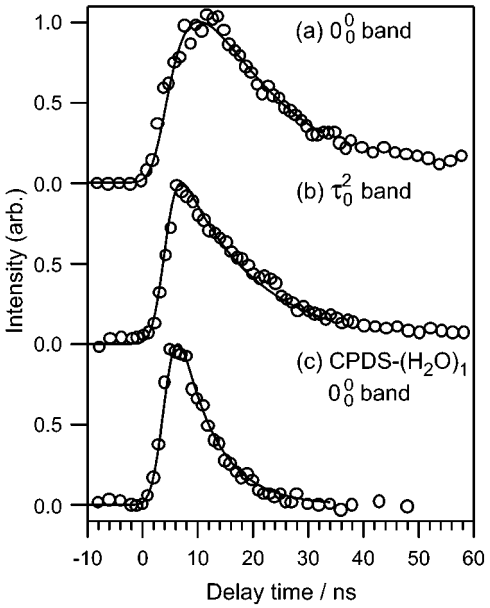

Figure 16. Temporal profile of the CT state population observed by a pump−probe technique using nanosecond pulse lasers. The bands excited are indicated in the figure. ○ represents experimental data, and − represents simulated data.

Table 3. Rise and Decay Time Constants of the CT State of CPDS

	CPDS (0_0^0)	CPDS (τ_0^2)	CPDS–$(H_2O)_1$ (0_0^0)
rise (λ_1/ns)	4	0	0
decay (λ_2/ns)	15	13.5	6.5

D. Time Domain Properties. Finally, time domain properties of the ICT process of CPDS and its cluster with water are briefly described. As discussed in section 3B, the proper selection of the laser wavelength of two-color RE2PI makes it possible to detect only the CT component in the electronic excited state, S_1. Thus, the temporal profile of the CT state emission can be recorded by changing the delay time between the excitation (pump) and ionization (probe) laser shots. Figure 16 shows the temporal profile of the CT state observed in the present method. The temporal profile of the CT state excited at the 0_0^0 band is well reproduced by a double exponential curve with a rise and a decay constant, which are listed in Table 3. As expected, the CT state rises slower in the case of the 0_0^0 band excitation than that in the case of the τ_0^2 band excitation.

Assuming a kinetic model schematically represented in Figure 17, the temporal profile of the CT state population in arbitrary unit, $I_{\mathrm{CT}}(t)$, can be expressed by a double exponential function

$$I_{\mathrm{CT}}(t) = \frac{k_{+\mathrm{CT}}\lambda_1\lambda_2}{\lambda_2-\lambda_1}\left\{\exp\left(-\frac{t}{\lambda_2}\right)-\exp\left(-\frac{t}{\lambda_1}\right)\right\}I_{\mathrm{LE}}^0 \qquad (4)$$

(40) Plitt, H. S.; Balaji, V.; Michl, J. *Chem. Phys. Lett.* **1993**, *213*, 158.

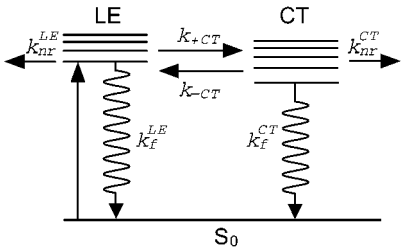

Figure 17. Kinetic model for the ICT process.

where I_{LE}^0 is an initial population of the LE state in arbitrary unit

$$\frac{1}{\lambda_{1,2}} = \frac{1}{2}(k_1 + k_2) \pm \frac{1}{2}\{(k_1 - k_2)^2 + 4k_{+CT}k_{-CT}\}^{1/2} \quad (5)$$

and

$$k_1 = k_f^{LE} + k_{nr}^{LE} + k_{+CT}, \quad k_2 = k_f^{CT} + k_{nr}^{CT} + k_{-CT} \quad (6)$$

Here, $k_f^{LE(CT)}$ and $k_{nr}^{LE(CT)}$ are rate constants for the fluorescence and the nonradiative decay in the LE (CT) state, respectively. The rate constants of the forward and backward CT processes are k_{+CT} and k_{-CT}, respectively. All of the rate constants, k, are in units of s^{-1}, while rise and decay time constants, λ, are in units of s. As listed in Table 3, the values of $\lambda_{1,2}$ are different for the 0_0^0 and the τ_0^2 excitation. Because the difference in energy between the 0^0 and the τ^2 levels is only 25 cm^{-1}, it is assumed that the values of $k_f^{LE(CT)}$ and $k_{nr}^{LE(CT)}$ are the same. On the other hand, the values of k_{+CT} and k_{-CT} for the 0^0 and the τ^2 levels should be significantly different. Unfortunately, there are not enough data to determine each rate constant which contains more physical meaning. In addition to the temporal profiles of the CPDS monomer, that of the CPDS$-(H_2O)_1$ cluster excited at its 0_0^0 band is also shown in Figure 16. It is apparent that the decay time constant, λ_2, becomes smaller as compared to those of the monomer cases. The reduction of the lifetime of the CT state by the solvent effect is also reported by the study in the solution.[22] Thus, the solvation with a single water molecule provides the similar feature of the decay processes of CPDS in solution, as well as the spectroscopic characterization by the solvation.

5. Concluding Remarks

In the present study, we have discussed the ICT process of the jet-cooled isolated CPDS monomer. The electronic configuration of the CT state is strongly suggested to be of the (σ_{Si-Si}, $2p\pi^*$) type by the fact that the ionization efficiency from the CT state is much better than that from the LE state. The intensity of the CT emission, that is, the CT state formation rate, is significantly dependent on the torsional motion of the disilanyl group with respect to the phenyl ring. On the basis of the electronic configuration of the LE and the CT states and the torsional angle dependence of the σ_{Si-Si} and π orbitals, it was revealed that the torsional motion is the promoting mode of the ICT process of CPDS. The vibrational dependence of the CT emission intensity was considered to reflect the overlap of wave functions between the LE and CT states. On the other hand, the accepting mode of the ICT process is considered to be a Si−Si stretching motion rather than the torsional motion. As discussed in the last paragraph of section 4C, attention is necessary to compare our result with the ICT process in condensed phases. Because our observation was carried out in the jet-cooled isolated molecular condition, the vibrational relaxation that occurs during the ICT process is the IVR relaxation; that is, there is no energy relaxation. The LE and CT states are mixed or interact with each other by the changes in the electronic wave function along the torsional coordinate of the disilanyl group. Although the present work leads us to a conclusion that the equilibrium geometry of the CT state along the torsional motion should be displaced from that of the LE state, a definitive determination of the equilibrium geometry of the CT state requires more detailed spectroscopic information, such as an observation of a direct excitation from the S_0 to the CT state.

Finally, we would like to briefly comment on the TICT problem. In the TICT model of DMABN, the torsional motion is considered to be both the accepting and the promoting modes. On the other hand, the torsional motion is the promoting mode but not the accepting mode in our CPDS case. Our results suggest that a twist of 90° is not necessary in the transition from the LE to the CT states even though the torsional motion is the promoting mode, since the ICT process occurs even in a zero point vibrational level in the LE state in the jet-cooled condition. In addition, the most distinct structural change during the ICT process of CPDS is an elongation of the Si−Si bond. Thus, the ICT process of CPDS is considered to be different from that of the TICT molecules. However, our results suggest that the necessity of the twisting between the electron-donating and -accepting groups does not necessarily mean that the most important structural change between the LE and the CT states is the twist of 90° for the ICT process of the TICT molecules.

Acknowledgment. The authors are very grateful to Dr. W. Setaka and Mr. T. Li in synthesizing the deuterated phenylpentamethyldisilane. One of the authors (H.I.) also thanks Mitsubishi Chemical Corp. Fund for financial support.

JA017753L